Published in final edited form as:

*Pediatr Res*. 2012 July ; 72(1): 2–9. doi:10.1038/pr.2012.32.

# Uteroplacental insufficiency alters rat hippocampal cellular phenotype in conjunction with ErbB receptor expression

**Camille Fung**[1], **Xingrao Ke**[1], **Ashley S. Brown**[1], **Xing Yu**[1], **Robert A. McKnight**[1], and **Robert H. Lane**[1]

[1]Department of Pediatrics, University of Utah School of Medicine, Salt Lake City, Utah 84105

## Abstract

**INTRODUCTION—**Uteroplacental insufficiency (UPI) produces significant neurodevelopmental deficits affecting the hippocampus of intrauterine growth restricted (IUGR) offspring. IUGR males have worse deficits compared to IUGR females. The exact mechanisms underlying these deficits are unclear. Alterations in hippocampal cellular composition along with altered expression of neural stem cell (NSC) differentiation molecules may underlie these deficits.

**HYPOTHESIS—**We hypothesized that IUGR hippocampi would be endowed with altered neuronal, astrocytic, and immature oligodendrocytic proportions at birth, with males showing greater cellular deficits. We further hypothesized that UPI would perturb rat hippocampal expression of ErbB receptors (ErbB-Rs) and Neuregulin 1 (NRG1) at birth and at weaning to account for the short- and long-term IUGR neurological sequelae.

**METHODS—**A well established rat model of bilateral uterine artery ligation at embryonic day (*E*) *19.5* was used to induce IUGR.

**RESULTS—**Compared to gender-matched controls, IUGR offspring have altered hippocampal neuronal, astrocytic, and immature oligodendrocytic composition in a subregion- and gender-specific manner at birth. In addition, IUGR hippocampi have altered receptor-type- and gender-specific ErbB-R expression at birth and at weaning.

**CONCLUSIONS—**These cellular and molecular alterations may account for the neurodevelopmental complications of IUGR and for the male susceptibility to worse neurologic outcomes.

## Introduction

Uteroplacental insufficiency (UPI) is the most common cause of intrauterine growth restriction (IUGR) of a fetus in developed countries and leads to short- and long-term neurodevelopmental disabilities in the offspring. These disabilities include tonal abnormalities, difficulties in working memory, recognition memory, visual spatial tasks,



Corresponding author: Camille Fung, M.D., P.O. Box 581289, Salt Lake City, UT 84158, Telephone: (801) 585-6287, Fax (801) 581-4724, camille.fung@hsc.utah.edu.

C.F. and X. K. contributed equally to this study.

behavior and concentration (1). Correlating with these functional deficits, neuroimaging has shown that hippocampal volume within the cortical gray matter is particularly reduced in human IUGR infants (2). In addition, IUGR male offspring demonstrate an increased severity of neurological impairment compared to IUGR female offspring (3, 4).

The exact mechanisms underlying IUGR-associated neurodevelopmental disabilities are unclear. Furthermore, the male susceptibility to worse neurologic function is not completely understood. Using a bilateral uterine artery ligation model to induce UPI in the rat, our laboratory has previously shown that juvenile IUGR male offspring at postnatal day (*P*) *21* have decreased myelin basic protein-to-neuronal nuclei ratio in all subregions of the hippocampus (CA1, CA3, and dentate gyrus, DG) (5). In contrast, neurons and synaptic density were preserved at *P21*. The current study aims to determine the effects of UPI on hippocampal neuronal, astrocytic, and immature oligodendrocytic composition at birth (*P0*) to determine whether IUGR offspring are born with a different cellular composition which then changes as the offspring matures.

A second aim of this study is to determine how UPI affects neural stem cells (NSCs), the progenitor cells that give rise to neurons and glia, when UPI is occurring. In particular, we will examine how UPI affects the molecules that govern NSC differentiation into neurons and glia. These molecules include the the ErbB receptors (ErbB-Rs) and their ligand, neuregulin 1 (NRG1). The ErbB receptor family includes ErbB2, ErbB3, and ErbB4. Once ErbB3 and ErbB4 bind to NRG1, they must heterodimerize with ErbB2 for cell fate regulation (6, 7). ErbB2 has no known endogenous ligand.

We therefore hypothesized that IUGR rat hippocampi would have decreased number of neurons, astrocytes, and immature oligodendrocytes at *P0*, with males showing greater cellular deficits. We further hypothesized that UPI would perturb rat hippocampal expression of ErbB-Rs and NRG1 at *P0* and *P21* to account for the short-and long-term cellular changes of IUGR. To test these hypotheses, we employed our rat model of bilateral uterine artery ligation to induce UPI, producing asymmetrical IUGR pups born 20–25% lighter in weight but with demonstrable cerebral alterations (8–11). We focused on the hippocampus in this study because this structure is intimately involved in learning and memory, is particular susceptible to metabolic disturbances such as UPI (1, 12), and harbors a NSC niche within the DG (13).

## Methods

University of Utah Animal Care Committee approved all procedures which were carried out in accordance with the National Institute of Health Guide for the Care and Use of Laboratory Animals. The rat model of UPI has been previously described (5, 14).

### Animal perfusion for histology

*P0* pups (n = 6/group from 3 separate control, CON, and 3 separate IUGR litters) were individually fixed via intracardiac perfusion with ice cold 0.9% normal saline (vWR, Radnor, PA), followed by ice cold 2% paraformaldehyde (Electron Microscopy Sciences, Hatfield, PA)/1.4% sodium cacodylate (Sigma-Aldrich, St. Louis, MO)/5% sucrose (vWR)

for 10 min. Dissected whole brains were post-fixed at 4°C overnight, cryoprotected with 15% and 30% sucrose at 4°C overnight, and embedded in 2% gelatin, 0.9% NaCl, 0.05% $NaN_3$ (Sigma-Aldrich) under freezing condition. They were sectioned coronally with a cryostat at 10 μm per section (Microm HM550, Microm International, Walldorf, Germany). Sections were collected sequentially on 10 consecutive Superfrost Plus slide (Fisher Scientific, Pittsburgh, PA) such that the 1st and every 10th section were on the same slide.

### Nissl stain to quantify dorsal hippocampal subregional volumes at *P0*

Sections encompassing the dorsal hippocampal were soaked in decreasing ethanol (vWR) baths. After 2 brief deionized $H_2O$ ($DH_2O$) washes, sections were incubated in cresyl violet stain (Sigma-Aldrich) (1.25 g cresyl violet acetate and 0.75 ml glacial acetic acid to 250 ml warm $DH_2O$) for 2 min and washed in $DH_2O$ for 1 min. Sections were dehydrated by a series of increasing ethanol baths and finally cleared by Histoclear (AGTC Bioproducts, Wilmington, MA) for 5 min. Sections were covered with mounting medium, coverslipped, and examined under light microscopy at 15x and 30x magnifications.

### Morphometric analyses of Nissl-stained dorsal hippocampi at *P0*

Hippocampal DG, CA3, and CA1 subregions of CON and IUGR groups at 30x magnification were outlined manually using NIH ImageJ software. Hippocampal subregional areas were calculated as a percentage of total hippocampal area. Since each section was 10 μm thick, we calculated each subregion's volume according to the Cavaleri Principle where $V=\Sigma A \times P \times t$ where V=total volume, ΣA=sum of measured areas, *P*=inverse of section sampling fraction, and *t* is section thickness (15). DG, CA3, and CA1 subregional volumes were generated for CON and IUGR groups.

### Immunofluorescent labeling of neurons with neuronal nuclear antigen (NeuN), of astrocytes with glial fibrillary acidic protein (GFAP), and of immature oligodendrocytes with O1 at *P0*

Sections were blocked with 3% normal goat serum (NGS)/0.05% Triton X-100 (Sigma-Aldrich) for 1 h at RT, incubated with mouse IgG monoclonal anti-NeuN antibody (MAB377, Millipore, Billerica, MA) at 1:1000, rabbit polyclonal anti-GFAP antibody (ab7779, Abcam, Cambridge, MA) at 1:2000, or mouse IgM monoclonal anti-immature oligodendrocyte marker O1 antibody (MAB1327, R&D systems, Minneapolis, MN) at 1:2000 in 3% NGS/0.05% Triton X-100 overnight at 4°C. Sections were washed three times in phosphate-buffered saline (PBS, Sigma-Aldrich) for 10 min and exposed to either secondary fluorescence-labeled DyLightTM 488-conjugated affinipure goat anti-mouse IgG at 1:1000, Cy-3-conjugated goat anti-rabbit at 1:1000, or DyLightTM 549-conjugated affinipure goat anti-mouse IgM at 1:2000 (Jackson ImmunoResearch, West Grove, PA) in 3% NGS/0.05% Triton X-100 for 1h at RT. Cell nuclei were counterstained with 10ng/ml DAPI (Molecular Probes, Invitrogen, Eugene, OR). Sections were washed again three times in PBS, air-dried, and coverslipped using Fluoromount-G mounting medium (Southern Biotech, Birmingham, AL). Negative control sections underwent similar staining procedure except for primary antibodies. Sections were imaged with the Olympus Fluoview FV1000 multiphoton laser scanning confocal microscope (Olympus Imaging America Inc, Center

Valley, PA) and taken at 10x and 20x magnification to encompass all subregions of the hippocampus (DG, CA3, and CA1).

### Morphometric analyses of immunofluorescent staining at *P0*

Sections encompassing the dorsal hippocampi at Bregma level ~−3.0 according to (16) were used for quantification. The number of NeuN positive ($NeuN^+$) neurons in DG, CA3, and CA1 was counted in the context of total $DAPI^+$ cells using NIH ImageJ software. Due to subregional hippocampal volume differences, DAPI count was normalized to the subregion with the fewest cells. Since GFAP and O1 largely stain for cell processes, we quantified the relative amount of astrocytes or immature oligodendrocytes by $GFAP^+$ or $O1^+$ staining divided by normalized $DAPI^+$ cell nuclei.

### Western immunoblotting for ErbB-Rs and NRG1 at *P0* and *P21*

Hippocampi were homogenized in ice cold RIPA buffer (n = 6/group with pups from 3 separate CON and 3 separate IUGR litters for each time point). Total protein concentration was determined by BCA Protein Assay (Pierce Biotechnology, Rockford, IL) using bovine serum albumin (Sigma-Aldrich) as standards. 100 μg of protein and molecular weight markers were separated by XT Criterion gel electrophoresis (Bio-Rad Laboratories, Hercules, CA) at 200 V for 1 h. After electrophoresis, proteins were transferred to polyvinylidene fluoride membranes (Millipore) overnight at 4°C. Post-transfer, membranes were blocked in 5% milk/Tris-buffered saline Tween (TBS-T) at RT for 1–1.5 h. Bound proteins were detected with antibodies against ErbB2 (ab2428, Abcam) 1:200 in 5% milk/TBS-T; ErbB3 (05–390, Millipore) 1:100 in 5% milk/TBS-T; ErbB4 (ab19391, Abcam) 1:100 in 5% milk/TBS-T; total NRG1 (ab2994, Abcam) 1:150 in 5% milk/TBS-T; GAPDH (2118, Cell Signaling Technology, Danvers, MA) 1:2000 in 5% milk/TBS-T at 4°C overnight. Membranes were probed with either horseradish peroxidase-conjugated anti-rabbit or anti-mouse IgG antibody at 1:2000–1:3000 in 5% milk (Cell Signaling) secondary antibody for 1 h at RT. Antibody signals were detected with Western Lighting enhanced chemiluminescence (PerkinElmer, Waltham, MA) and quantified with Kodak Image Station 2000R (Eastman Kodak/SIS, Rochester, NY). GAPDH served as loading control. Hippocampal GAPDH protein expression was determined to be unaltered in our IUGR model (data not shown).

### Statistics

Immunofluorescent histochemical quantification of NeuN, GFAP, and O1, normalized to CON females to highlight gender differences, is expressed as absolute values in arbitrary units. Protein levels of ErbB receptors and NRG-1 are expressed as means ± SEMs which were also normalized to CON females. Data were analyzed with ANOVA using Tukey *post hoc* test for equal sample sizes. Statistical significance was declared at $p<0.05$.

## Results

### Dorsal hippocampal subregional volumes in CON and IUGR animals at *P0*

IUGR significantly decreased female DG volume at *P0* compared to CON females (Fig. 1). IUGR, on the other hand, significantly decreased CA1 volume in males at *P0* compared to

CON males (Fig. 1). CON female and CON male hippocampal subregional volumes were similar (Fig 1).

### Hippocampal neurons, astrocytes, and immature oligodendrocytes in control and IUGR animals at *P0*

In the DG, CON males had a baseline decrease in neuron number compared to CON females (Fig 3). IUGR decreased neuron number in the DG in females only (Figs. 2A, 3). In contrast, IUGR decreased the number of neurons in CA3 and CA1 regions in males only (Figs. 2B, 2C, 3).

Similar to DG neurons, CON males had a baseline decrease in the amount of astrocytes compared to CON females (Fig. 4). IUGR increased the amount of DG astrocytes in males only (Figs. 2D, 4). On the other hand, IUGR decreased the amount of CA3 astrocytes in males only (Figs. 2E, 4). IUGR did not significantly affect CA1 astrocytes in either gender (Fig. 4).

Lastly, IUGR did not significantly alter the amount of immature oligodendrocytes in DG or CA3 in either gender (Fig 5). IUGR significantly increased the amount of CA1 immature oligodendrocytes in females (Fig. 2F, 5) but decreased the amount of CA1 immature oligodendrocytes in males (Fig 5).

### Hippocampal ErbB2 protein levels at *P0* and *P21*

IUGR females at *P0* increased hippocampal ErbB2 protein level compared to CON females (Fig. 6). On the other hand, IUGR males at *P0* had similar ErbB2 protein levels as CON males. CON female and male had similar ErbB2 protein levels at baseline. At *P21*, CON males had an increased baseline ErbB2 protein level compared to CON females (Fig. 6). IUGR did not alter ErbB2 protein levels in either gender at this age (Fig. 6).

### Hippocampal ErbB3 protein levels at *P0* and *P21*

IUGR males and females at *P0* decreased ErbB3 protein levels compared to gender-matched CON (Fig. 6). CON female and male had similar ErbB3 protein levels at baseline. At *P21*, CON males had increased baseline ErbB3 protein level over CON females, similar to ErbB2 protein expression (Fig. 6). IUGR males showed a further increase in ErbB3 protein level over CON males.

### Hippocampal ErbB4 protein levels at *P0* and *P21*

At *P0*, CON males show an increased baseline ErbB4 protein level over CON females. IUGR did not alter ErbB4 protein levels in either gender at *P0* (Fig. 7). IUGR also did not affect ErbB4 protein levels in either gender at *P21* (Fig. 7).

### Hippocampal NRG1 protein levels at *P0* and *P21*

At *P0* and *P21*, IUGR females and males had similar hippocampal NRG1 protein levels as their age- and gender-matched CON (Fig. 7). Additionally, CON males at *P21* had an increased NRG1 protein level compared to CON females (Fig. 7).

## Discussion

The most important finding of this study is that an acute UPI insult alters hippocampal neuronal, astrocytic, and immature oligodendrocytic composition in the rat IUGR offspring at birth in a region- and gender-specific manner. Along with altered hippocampal cellular composition, ErbB receptor expression is also altered in a receptor- and gender-specific manner. Collectively, these data provide a link of how the altered IUGR hippocampal cellular phenotype may result from altered NSC differentiation molecules such as the ErbB-R.

In our model, IUGR rat offspring showed a decrease in hippocampal neuron number at birth. This neuronal decrease is consistent with neuronal decreases observed in other animals of UPI (17, 18). However, important differences in our finding compared to these studies are in the region- and gender-specificity of these neuronal changes. While other models have shown decreased number of neurons within one brain region only, i.e. in the cerebral cortex or hippocampal CA1, our investigation separated the three main subregions of the hippocampus to highlight regional differences. Additionally, we separated our analyses based on gender in an attempt to understand whether being an IUGR male or female would portend different outcomes. What we found was that IUGR decreased hippocampal CA1 and CA3 neurons, while IUGR females decreased DG neurons.

Possible explanations for such region- and gender-specific neuronal decreases are multiple. CA1 and CA3 neurons arise separately by location and timing from the DG neurons during embryonic life. CA1 and CA3 neurons which originate from the Ammonic neuroepithelium are produced mostly on *E17* to *E20* in the rat brain. DG neurons which originate from the dentate neuroepithelium are produced mostly on *E18* to *E22* (19, 20). The molecular control governing these morphogenetic events is also known to be region-specific (21). Additionally, neurons in hippocampal subregions possess different intrinsic vulnerability to injury. A recent study demonstrated that prenatal stress (PNS) in pregnant rats elicited increased spine density on CA1 pyramidal neurons in male pups only (22). Furthermore, PNS altered DG granular neuron spine-density, dendritic length and complexity in opposite directions in male and female offspring. Together, neurons from different brain regions and from different genders will behave differently in response to an insult because of their inherent region and sex-autonomous differences.

Another explanation for our observed region- and gender-specificity may relate to the fact that neurons in IUGR male hippocampi are exposed to an environment of testosterone-estradiol imbalance. We have previously shown that our IUGR males at birth have increased serum testosterone level in association with decreased hippocampal aromatase expression while IUGR females do not (23). Aromatase is the enzyme responsible for the conversion of testosterone to its metabolite estradiol. The exposure of the developing brain to a balanced testosterone and estradiol ratio is critical for proper neuronal development (24). Therefore, over-exposure of the earlier formed CA1 and CA3 neurons to an excess of testosterone in our IUGR male rats may account for the selective regional neuronal loss.

In addition to neuronal decreases, UPI elicited region- and gender-specific astrocytic and immature oligodendrocytic changes at birth. Important to highlight here is that unlike neurons, IUGR males possessed opposing amounts of astrocytes in CA1 and CA3 regions of the rat hippocampus compared to control males. Opposing astrocytic amount in other chronic insults of UPI have been demonstrated in the cortices of guinea pigs and rabbits (25, 26). But the opposing astrocytic amount within subregions of one brain structure has not been seen previously. The etiology of these astrocytic differences remains unclear. We speculate that some of our explanations pertaining to the subregional neuronal differences may account for the subregional differences observed in astrocytes as well.

In terms of our findings with immature oligodendrocytes, UPI in this model produced a strong gender difference in the hippocampal CA1 region. Of importance to highlight is that IUGR males had decreased amount of immature oligodendrocytes at birth. From our previous work, IUGR males had decreased amount of myelin basic protein-to-neuronal nuclei ratio in the same region at *P21* (5). The current finding adds to the previous result by suggesting that the reduction in CA1 oligodendrocytic precursors at birth reduced the capacity to generate mature myelin basic protein at *P21*. Such an overall reduction in CA1 myelin basic protein will negatively affect the hippocampal function of IUGR males in the long term as CA1 neurons are responsible for sending the main hippocampal output back to the cortex for information processing (27).

The region- and gender-specific neuronal and glial changes observed in our model suggest that NSC differentiation is altered by UPI. ErbB receptors and their ligand, NRG1, are known to play critical roles in neuronal and glial development from NSCs (6, 28). Mice deficient in ErbB2, 3, or 4 receptor have all died at relatively early stages of development, making a complete analysis of the central nervous system phenotype difficult. ErbB2 null mice show marked abnormalities of their cranial ganglia (29), while ErbB4 null mice have abnormal innervation of the brainstem (30). Furthermore, ErbB receptors are known to be localized in NSCs of both rodents and humans (31–33). Within the germinal epithelia of the developing Sprague-Dawley rat brain, ErbB2 and ErbB4 mRNAs have been found to be widely distributed as early as *E12* (31). As rat brain development progressed, ErbB2 mRNA was mainly confined to the cells of the ventricular zone, while ErbB4 mRNA was mainly localized to the cells of the subventricular zone. These zones represent NSC niches in the developing and adult brain.

In our current study, IUGR females at birth decreased hippocampal ErbB3 receptor despite no change in NRG1 ligand expression. Hippocampal ErbB3 receptor decrease occurs in conjunction with ErbB2 receptor increase. Since ErbB3 receptor lacks intrinsic kinase activity and must heterodimerize with ErbB2 for downstream signaling (34), the increase in ErbB2 receptor may signify a compensatory response to the IUGR decrease in ErbB3 level. Interestingly, IUGR males also showed decreased hippocampal ErbB3 receptor at birth but they lacked the ErbB2 receptor upregulation. Such a lack of ErbB2 receptor compensation may suggest that IUGR males are more susceptible to aberrant hippocampal morphogenesis due to their inability to transmit extracellular NRG1 signal for proper hippocampal NSC differentiation. This speculation is in part supported by the ErbB3 mutant mice who have a

misshapened cerebellar plate that is poorly differentiated and contains fewer Purkinje cells compared to the wild-type (35).

We understand that limitations to our study exist. We have only examined total NRG1 expression. NRG1 has at least 15 known isoforms arising from alternative promoter usage and RNA splicing; therefore other NRG1 isoforms may be altered as a result of UPI. Another limitation is the mixed population of NSCs, neurons, and glia within the rat hippocampus. Ideally, isolating NSCs from the hippocampus would generate a more cell-type specific NRG1 and ErbB receptor expression profile. Future studies using the NSC-specific nestin-green fluorescent protein transgenic mice will help to isolate a pure population of NSCs to elucidate the NSC-specific changes in ErbB receptor and NRG1.

In conclusion, our study has delineated for the first time the natal hippocampal neuronal and glial phenotype in a model of UPI that has been in use since the 1960s. Given the current recognition of how many adult-onset neurocognitive and neuropsychiatric disorders may have origins in fetal life (36, 37), understanding how UPI affects the cellular makeup at birth and over time will open up mechanistic questions to address aberrant neural function in these IUGR offspring.

## Acknowledgments

Statement of financial support: This research was supported by National Institute of Child Health and Human Development Grant R01-HD-41075 (to R. H. Lane) and University of Utah Children's Health Research Career Development Award 5K12-HD001410-06 (to C. Fung).

We would like to thank Drs. Scott Rogers and Lorise Gahring for their expertise and guidance in immunofluorescent histochemistry and Dr. Christopher Rodesch for his expertise in immunofluorescent histochemical quantification.

## References

1. van Wassenaer A. Neurodevelopmental consequences of being born SGA. Pediatr Endocrinol Rev. 2005; 2:372–7. [PubMed: 16429113]
2. Tolsa CB, Zimine S, Warfield SK, et al. Early alteration of structural and functional brain development in premature infants born with intrauterine growth restriction. Pediatr Res. 2004; 56:132–8. [PubMed: 15128927]
3. Jarvis S, Glinianaia SV, Torrioli MG, et al. Cerebral palsy and intrauterine growth in single births: European collaborative study. Lancet. 2003; 362:1106–11. [PubMed: 14550698]
4. Lahti J, Raikkonen K, Kajantie E, et al. Small body size at birth and behavioural symptoms of ADHD in children aged five to six years. J Child Psychol Psychiatry. 2006; 47:1167–74. [PubMed: 17076756]
5. Schober ME, McKnight RA, Yu X, Callaway CW, Ke X, Lane RH. Intrauterine growth restriction due to uteroplacental insufficiency decreased white matter and altered NMDAR subunit composition in juvenile rat hippocampi. Am J Physiol Regul Integr Comp Physiol. 2009; 296:R681–92. [PubMed: 19144756]
6. Buonanno A, Fischbach GD. Neuregulin and ErbB receptor signaling pathways in the nervous system. Curr Opin Neurobiol. 2001; 11:287–96. [PubMed: 11399426]
7. Shah NM, Marchionni MA, Isaacs I, Stroobant P, Anderson DJ. Glial growth factor restricts mammalian neural crest stem cells to a glial fate. Cell. 1994; 77:349–60. [PubMed: 7910115]
8. Lane RH, Kelley DE, Gruetzmacher EM, Devaskar SU. Uteroplacental insufficiency alters hepatic fatty acid-metabolizing enzymes in juvenile and adult rats. Am J Physiol Regul Integr Comp Physiol. 2001; 280:R183–90. [PubMed: 11124150]

9. Ke X, McKnight RA, Wang ZM, et al. Nonresponsiveness of cerebral p53-MDM2 functional circuit in newborn rat pups rendered IUGR via uteroplacental insufficiency. Am J Physiol Regul Integr Comp Physiol. 2005; 288:R1038–45. [PubMed: 15563574]
10. Ke X, Lei Q, James SJ, et al. Uteroplacental insufficiency affects epigenetic determinants of chromatin structure in brains of neonatal and juvenile IUGR rats. Physiol Genomics. 2006; 25:16–28. [PubMed: 16380407]
11. Lane RH, Ramirez RJ, Tsirka AE, et al. Uteroplacental insufficiency lowers the threshold towards hypoxia-induced cerebral apoptosis in growth-retarded fetal rats. Brain Res. 2001; 895:186–93. [PubMed: 11259777]
12. Lodygensky GA, Seghier ML, Warfield SK, et al. Intrauterine growth restriction affects the preterm infant's hippocampus. Pediatr Res. 2008; 63:438–43. [PubMed: 18356754]
13. Parent JM. Injury-induced neurogenesis in the adult mammalian brain. Neuroscientist. 2003; 9:261–72. [PubMed: 12934709]
14. Baserga M, Hale MA, Wang ZM, et al. Uteroplacental insufficiency alters nephrogenesis and downregulates cyclooxygenase-2 expression in a model of IUGR with adult-onset hypertension. Am J Physiol Regul Integr Comp Physiol. 2007; 292:R1943–55. [PubMed: 17272666]
15. Gundersen HJ, Jensen EB. The efficiency of systematic sampling in stereology and its prediction. J Microsc. 1987; 147:229–63. [PubMed: 3430576]
16. Paxinos, GWC. The rat brain in stereotaxic coordinates. 4. San Diego: Academic Press; 1998.
17. Tashima L, Nakata M, Anno K, Sugino N, Kato H. Prenatal influence of ischemia-hypoxia-induced intrauterine growth retardation on brain development and behavioral activity in rats. Biol Neonate. 2001; 80:81–7. [PubMed: 11474155]
18. Mallard C, Loeliger M, Copolov D, Rees S. Reduced number of neurons in the hippocampus and the cerebellum in the postnatal guinea-pig following intrauterine growth-restriction. Neuroscience. 2000; 100:327–33. [PubMed: 11008170]
19. Altman J, Bayer SA. Mosaic organization of the hippocampal neuroepithelium and the multiple germinal sources of dentate granule cells. J Comp Neurol. 1990; 301:325–42. [PubMed: 2262594]
20. Altman J, Bayer SA. Migration and distribution of two populations of hippocampal granule cell precursors during the perinatal and postnatal periods. J Comp Neurol. 1990; 301:365–81. [PubMed: 2262596]
21. Li G, Pleasure SJ. Genetic regulation of dentate gyrus morphogenesis. Prog Brain Res. 2007; 163:143–52. [PubMed: 17765716]
22. Bock J, Murmu MS, Biala Y, Weinstock M, Braun K. Prenatal stress and neonatal handling induce sex-specific changes in dendritic complexity and dendritic spine density in hippocampal subregions of prepubertal rats. Neuroscience. 2011; 193:34–43. [PubMed: 21807071]
23. O'Grady SP, Caprau D, Ke XR, et al. Intrauterine growth restriction alters hippocampal expression and chromatin structure of Cyp19a1 variants. Syst Biol Reprod Med. 2010; 56:292–302. [PubMed: 20662593]
24. Schwarz JM, McCarthy MM. Steroid-induced sexual differentiation of the developing brain: multiple pathways, one goal. J Neurochem. 2008; 105:1561–72. [PubMed: 18384643]
25. Nitsos I, Rees S. The effects of intrauterine growth retardation on the development of neuroglia in fetal guinea pigs. An immunohistochemical and an ultrastructural study. Int J Dev Neurosci. 1990; 8:233–44. [PubMed: 1696773]
26. Bassan H, Kidron D, Bassan M, et al. The effects of vascular intrauterine growth retardation on cortical astrocytes. J Matern Fetal Neonatal Med. 2010; 23:595–600. [PubMed: 19757337]
27. Kealy J, Commins S. The rat perirhinal cortex: A review of anatomy, physiology, plasticity, and function. Prog Neurobiol. 2011; 93:522–48. [PubMed: 21420466]
28. Yarden Y, Sliwkowski MX. Untangling the ErbB signalling network. Nat Rev Mol Cell Biol. 2001; 2:127–37. [PubMed: 11252954]
29. Lee KF, Simon H, Chen H, Bates B, Hung MC, Hauser C. Requirement for neuregulin receptor erbB2 in neural and cardiac development. Nature. 1995; 378:394–8. [PubMed: 7477377]
30. Gassmann M, Casagranda F, Orioli D, et al. Aberrant neural and cardiac development in mice lacking the ErbB4 neuregulin receptor. Nature. 1995; 378:390–4. [PubMed: 7477376]

31. Kornblum HI, Yanni DS, Easterday MC, Seroogy KB. Expression of the EGF receptor family members ErbB2, ErbB3, and ErbB4 in germinal zones of the developing brain and in neurosphere cultures containing CNS stem cells. Dev Neurosci. 2000; 22:16–24. [PubMed: 10657694]

32. Fox IJ, Kornblum HI. Developmental profile of ErbB receptors in murine central nervous system: implications for functional interactions. J Neurosci Res. 2005; 79:584–97. [PubMed: 15682390]

33. Chong VZ, Webster MJ, Rothmond DA, Weickert CS. Specific developmental reductions in subventricular zone ErbB1 and ErbB4 mRNA in the human brain. Int J Dev Neurosci. 2008; 26:791–803. [PubMed: 18662768]

34. Esper RM, Pankonin MS, Loeb JA. Neuregulins: versatile growth and differentiation factors in nervous system development and human disease. Brain Res Rev. 2006; 51:161–75. [PubMed: 16412517]

35. Erickson SL, O'Shea KS, Ghaboosi N, et al. ErbB3 is required for normal cerebellar and cardiac development: a comparison with ErbB2-and heregulin-deficient mice. Development. 1997; 124:4999–5011. [PubMed: 9362461]

36. Joss-Moore LA, Lane RH. The developmental origins of adult disease. Curr Opin Pediatr. 2009; 21:230–4. [PubMed: 19663040]

37. Entringer S, Buss C, Wadhwa PD. Prenatal stress and developmental programming of human health and disease risk: concepts and integration of empirical findings. Curr Opin Endocrinol Diabetes Obes. 2010; 17:507–16. [PubMed: 20962631]

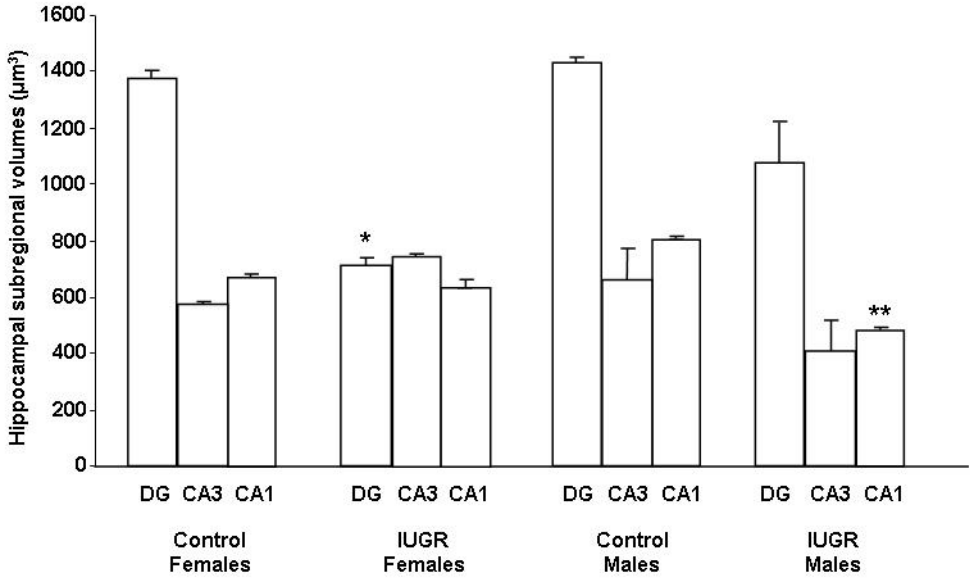


**Figure 1. Quantification of dorsal hippocampal DG, CA3, and CA1 subregional volumes at *P0***

Hippocampal subregional volumes are depicted as means ± SEMs in $\mu m^3$. n = 6/group. *p<0.05 vs. Control Females DG, **p<0.05 vs. Control Males CA1.

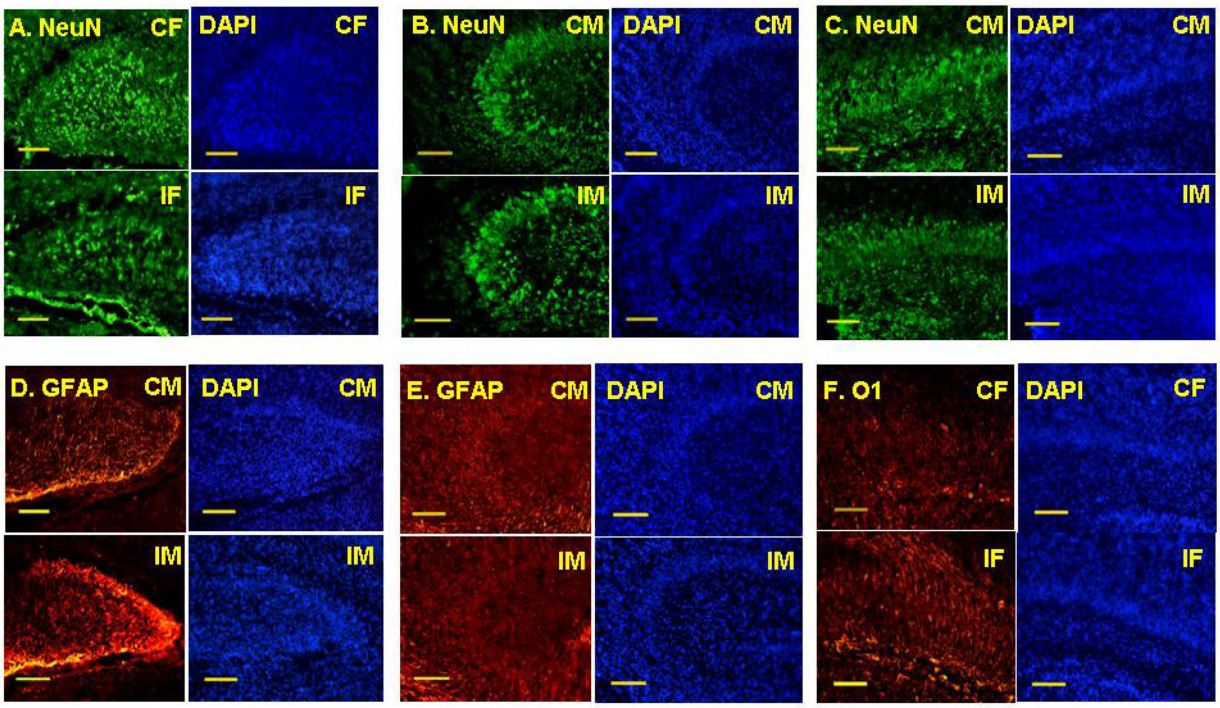


**Figure 2. NeuN, GFAP, and O1 immunofluorescent staining for neurons, astrocytes, and immature oligodendrocytes respectively in CON and IUGR hippocampal DG, CA3, and CA1 subregions at *P0***

Representative hippocampal NeuN and DAPI immunofluorescent microscopic images from DG (A) of Control Females (CF) and IUGR Females (IF), from CA3 (B) and CA1 (C) of Control Males (CM) and IUGR Males (IM). Representative hippocampal GFAP and DAPI immunofluorescent microscopic images from DG (D) and CA3 (E) of CM and IM. Representative hippocampal O1 and DAPI immunofluorescent microscopic images from CA1 (F) of CF and IF. n = 6/group. Scale bars represent 50μm.

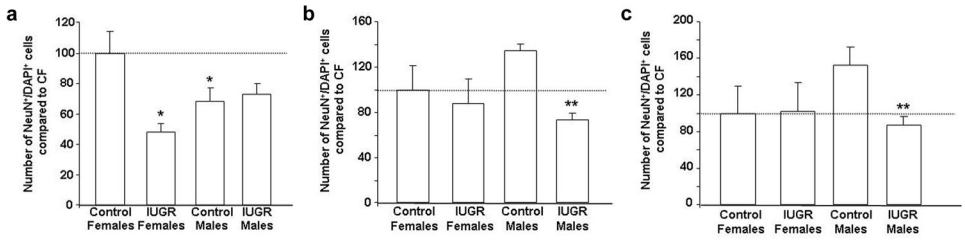


**Figure 3. Quantification of neuron number in CON and IUGR hippocampal subregions at *P0***

Quantification of neuron number in hippocampal DG (A), CA3 (B) and CA1 (C). Data are normalized to Control Females (CF) set at 100%. *p<0.05 vs. Control Females, **p<0.05 vs. Control Males.

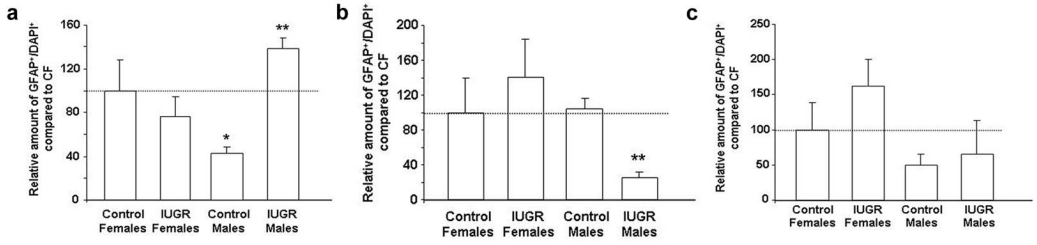


**Figure 4. Quantification of relative amount of astrocytes in CON and IUGR hippocampal subregions at *P0***

Quantification of relative amount of astrocytes in hippocampal DG (A), CA3 (B), and CA1 (C). Data are normalized to Control Females (CF) set at 100%. *p<0.05 vs. Control Females, **p<0.05 vs. Control Males.

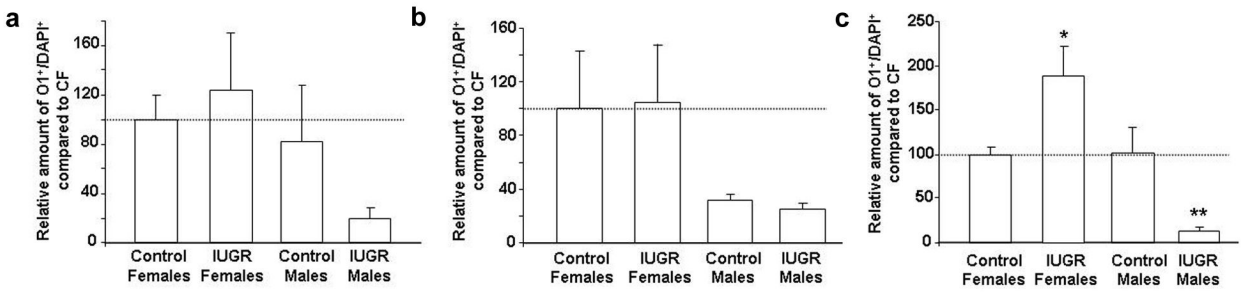


**Figure 5. Quantification of relative amount of immature oligodendrocytes in CON and IUGR hippocampal subregions at *P0***

Quantification of relative amount of immature oligodendrocytes in hippocampal DG (A), CA3 (B), and CA1 (C). Data are normalized to Control Females (CF) set at 100%. *p<0.05 vs. Control Females, **p<0.05 vs. Control Males.

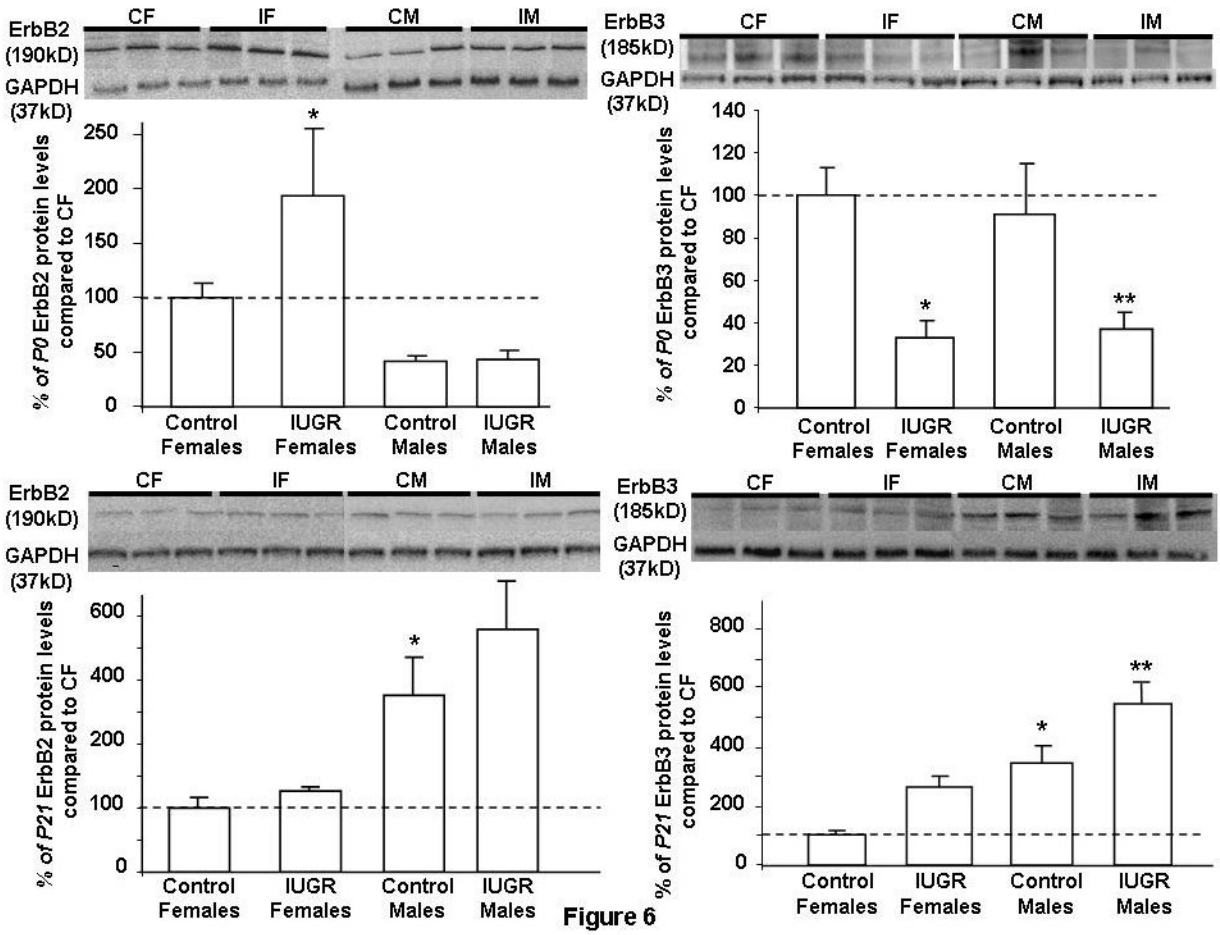


**Figure 6. Quantification of hippocampal ErbB2 and ErbB3 protein levels at *P0* and *P21***

Results are depicted as %means ± SEMs compared to Control Females set as 100% (n = 6/group/time point). Representative Western blots are depicted above the Western quantification. Control Females (CF); IUGR Females (IF); Control Males (CM); IUGR Males (IM). GAPDH acted as loading control. *p<0.05 vs. Control Females, **p<0.05 vs. Control Males.

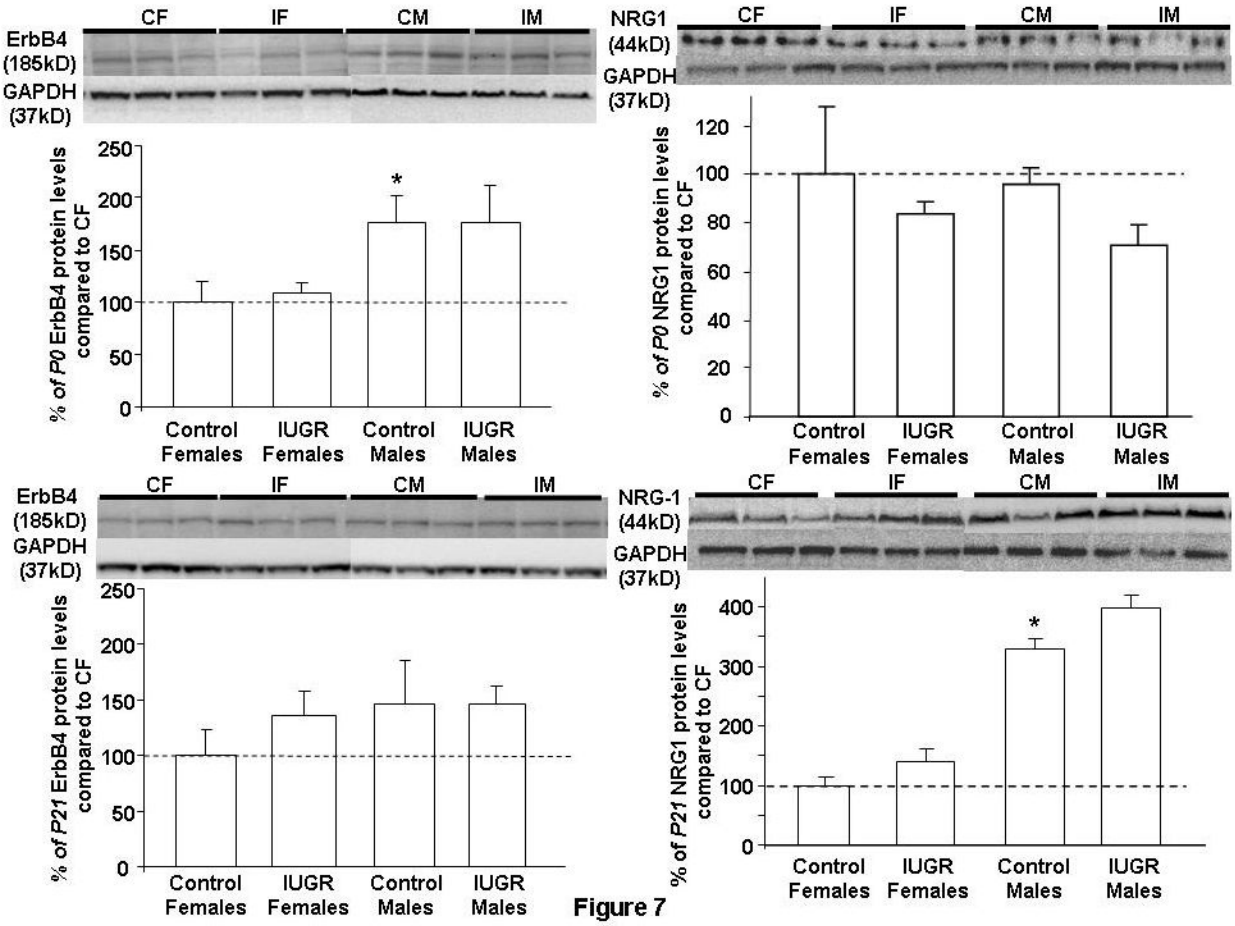


**Figure 7. Quantification of hippocampal ErbB4 and NRG1 protein levels at *P0* and *P21***

Results are depicted as % means ± SEMs compared to Control Females set as 100% (n = 6/group/time point). Representative Western blots are depicted above the Western quantification. Control Females (CF); IUGR Females (IF); Control Males (CM); IUGR Males (IM). GAPDH acted as loading control. *p<0.05 vs. Control Females.